Siberian Branch of Russian Academy of Science

BUDKER INSTITUTE OF NUCLEAR PHYSICS

R.R.Akhmetshin, E.V.Anashkin, M.Arpagaus, V.M.Aulchenko,
V.S.Banzarov, L.M.Barkov, N.S.Bashtovoy, A.E.Bondar,
D.V.Bondarev, A.V.Bragin, D.V.Chernyak, A.S.Dvoretsky,
S.I.Eidelman, G.V.Fedotovich, N.I.Gabyshev, A.A.Grebeniuk,
D.N.Grigoriev, P.M.Ivanov, S.V.Karpov, V.F.Kazanin,
B.I.Khazin, I.A.Koop, P.P.Krokovny, L.M.Kurdadze,
A.S.Kuzmin, I.B.Logashenko, P.A.Lukin, A.P.Lysenko,
K.Yu.Mikhailov, I.N.Nesterenko, V.S.Okhapkin,
E.A.Perevedentsev, E.A.Panich, A.S.Popov, T.A.Purlatz,
N.I.Root, A.A.Ruban, N.M.Ryskulov, A.G.Shamov,
Yu.M.Shatunov, B.A.Shwartz, A.L.Sibidanov, V.A.Sidorov,
A.N.Skrinsky, V.P.Smakhtin, I.G.Snopkov, E.P.Solodov,
P.Yu.Stepanov, A.I.Sukhanov, V.M.Titov, J.A.Thompson,
Yu.V.Yudin, S.G.Zverev

STUDY OF THE ϕ DECAYS INTO $\pi^+\pi^-\gamma$, $\pi^0\pi^0\gamma$ AND $\eta\pi^0\gamma$ FINAL STATES

Budker INP 99-51

http://www.inp.nsk.su/publications

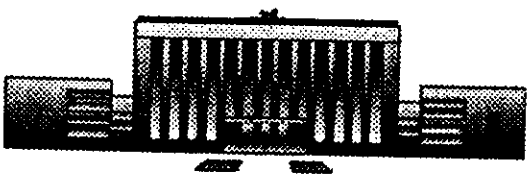

Novosibirsk
1999

Siberian Branch of Russian Academy of Science
BUDKER INSTITUTE OF NUCLEAR PHYSICS

R.R.Akhmetshin, E.V.Anashkin, M.Arpagaus, V.M.Aulchenko,
V.S.Banzarov, L.M.Barkov, N.S.Bashtovoy, A.E.Bondar, D.V.Bondarev,
A.V.Bragin, D.V.Chernyak, A.S.Dvoretsky, S.I.Eidelman, G.V.Fedotovich,
N.I.Gabyshev, A.A.Grebeniuk, D.N.Grigoriev, P.M.Ivanov, S.V.Karpov,
V.F.Kazanin, B.I.Khazin, I.A.Koop, P.P.Krokovny, L.M.Kurdadze,
A.S.Kuzmin, I.B.Logashenko, P.A.Lukin, A.P.Lysenko, K.Yu.Mikhailov,
I.N.Nesterenko, V.S.Okhapkin, E.A.Perevedentsev, E.A.Panich, A.S.Popov,
T.A.Purlatz, N.I.Root, A.A.Ruban, N.M.Ryskulov, A.G.Shamov,
Yu.M.Shatunov, B.A.Shwartz, A.L.Sibidanov, V.A.Sidorov, A.N.Skrinsky,
V.P.Smakhtin, I.G.Snopkov, E.P.Solodov, P.Yu.Stepanov, A.I.Sukhanov,
V.M.Titov, J.A.Thompson, Yu.V.Yudin, S.G.Zverev

STUDY OF THE ϕ DECAYS INTO $\pi^+\pi^-\gamma$, $\pi^0\pi^0\gamma$ AND $\eta\pi^0\gamma$ FINAL STATES

Budker INP 99-51

NOVOSIBIRSK
1999

STUDY OF THE ϕ DECAYS INTO $\pi^+\pi^-\gamma$, $\pi^0\pi^0\gamma$ AND $\eta\pi^0\gamma$ FINAL STATES

R.R.Akhmetshin, E.V.Anashkin, M.Arpagaus, V.M.Aulchenko, V.S.Banzarov, L.M.Barkov, N.S.Bashtovoy, A.E.Bondar, D.V.Bondarev, A.V.Bragin, D.V.Chernyak, A.S.Dvoretsky, S.I.Eidelman, G.V.Fedotovich, N.I.Gabyshev, A.A.Grebeniuk, D.N.Grigoriev, P.M.Ivanov, S.V.Karpov, V.F.Kazanin, B.I.Khazin, I.A.Koop, P.P.Krokovny, L.M.Kurdadze, A.S.Kuzmin, I.B.Logashenko, P.A.Lukin, A.P.Lysenko, K.Yu.Mikhailov, I.N.Nesterenko, V.S.Okhapkin, E.A.Perevedentsev, E.A.Panich, A.S.Popov, T.A.Purlatz, N.I.Root, A.A.Ruban, N.M.Ryskulov, A.G.Shamov, Yu.M.Shatunov, B.A.Shwartz, A.L.Sibidanov, V.A.Sidorov, A.N.Skrinsky, V.P.Smakhtin, I.G.Snopkov, E.P.Solodov, P.Yu.Stepanov, A.I.Sukhanov, V.M.Titov, Yu.V.Yudin, S.G.Zverev

Budker Institute of Nuclear Physics
630090 Novosibirsk, Russia

J.A.Thompson

University of Pittsburgh, Pittsburgh, PA 15260, USA

Abstract

Radiative decays of the ϕ meson have been studied using a data sample of about 20 million ϕ decays collected by the CMD-2 detector at VEPP-2M collider in Novosibirsk. From selected $e^+e^- \to \pi^0\pi^0\gamma$ and $e^+e^- \to \eta\pi^0\gamma$ events the following model independent results have been obtained:
$Br\phi \to \pi^0\pi^0\gamma) = (0.92 \pm 0.08 \pm 0.06) \times 10^{-4}$ for $M_{\pi^0\pi^0} > 700$ MeV,
$Br(\phi \to \eta\pi^0\gamma) = (0.90 \pm 0.24 \pm 0.10) \times 10^{-4}$.

It is shown that the intermediate mechanism $f_0(980)\gamma$ dominates in the $\phi \to \pi^+\pi^-\gamma$ and $\phi \to \pi^0\pi^0\gamma$ decays and the corresponding branching ratio is $Br(\phi \to f_0(980)\gamma) = (3.11 \pm 0.23) \times 10^{-4}$.

Selected $e^+e^- \to \mu^+\mu^-\gamma$ events were used to obtain
$Br(\phi \to \mu^+\mu^-\gamma) = (1.43 \pm 0.45 \pm 0.14) \times 10^{-5}$ for $E_\gamma > 20$ MeV.

Using the same data sample upper limits have been obtained for the C-violating decay of the ϕ:

$Br(\phi \to \rho\gamma) < 1.2 \times 10^{-5}$; and for the P- and CP-violating decays of the η at 90% CL:

$Br(\eta \to \pi^+\pi^-) < 3.3 \times 10^{-4}$,

$Br(\eta \to \pi^0\pi^0) < 4.3 \times 10^{-4}$.

Introduction

The electric dipole radiative decays of the ϕ meson are very interesting for the clarification of the nature of $f_0(980)$ and $a_0(980)$ mesons [1]. A search for these decays has been earlier performed by the ND group [2] and a number of new results has been recently published by SND [3,4] and CMD-2 [5,6] collaborations at the e^+e^- collider VEPP-2M [7] where the radiative decays $\phi \to \pi^0\pi^0\gamma$, $\phi \to \eta\pi^0\gamma$ and $\phi \to \pi^+\pi^-\gamma$ have been observed for the first time.

The mode with two charged pions has very large background because of the radiative processes $e^+e^- \to \pi^+\pi^-\gamma$ where a photon comes from initial electrons or from final pions. Therefore a signal from the $f_0(980)\gamma$ final state is seen as an interference structure at the energy $E_\gamma = \frac{m_\phi^2 - m_{f_0}^2}{2m_\phi} \approx 40$ MeV in the photon spectrum. The shape of this structure depends on the $f_0(980)$ mass and width. In our first paper [8] a search for the $\phi \to \pi^+\pi^-\gamma$ decay led to the upper limit of 3×10^{-5} that looked puzzlingly low compared to the decay $\phi \to \pi^0\pi^0\gamma$ observed with the branching ratio of about 1×10^{-4} [4]. As it was shown in [5,8,9], in case of the $f_0(980)\gamma$ mechanism it could be explained by the destructive interference between bremsstrahlung processes and the ϕ decay.

The purely neutral mode has no bremsstrahlung background and is the most efficient to study the $\phi \to f_0(980)\gamma$ decay and two pion mass spectrum. With the CMD-2 detector this mode as well as another ϕ decay with five photons in the final state $\phi \to \eta\pi^0\gamma$ have been studied and the first results [5] based on about 25% of the data confirmed those reported earlier by SND.

The CMD-2 detector described in detail elsewhere [10] has been taking data since 1992. In addition to the barrel CsI calorimeter, the endcap calorimeter made of BGO crystals was installed in 1995 making detector almost hermetic to the photons. The energy resolution for photons in the CsI calorimeter is about 8% independent of the energy and $\sigma_E/E = 4.6\%/\sqrt{E(GeV)}$ for the BGO calorimeter. The muon system uses streamer tubes grouped in two layers (inner and outer) with a 15 cm magnet yoke serving as an absorber and has 1-3 cm spatial resolution.

In this paper results of the study of the $\phi \to \pi^0\pi^0\gamma$, $\phi \to \pi^+\pi^-\gamma$ and $\phi \to \eta\pi^0\gamma$ are presented. In total the 14.2 pb^{-1} of data have been collected at 14 energy points around the ϕ mass and correspond to 20.6×10^6 of ϕ decays. For this analysis 13.1 and 12.8 pb^{-1} were used for the $\pi^+\pi^-\gamma$ and $\pi^0\pi^0\gamma$ decay modes respectively. Seven scans of this energy region were performed allowing to control systematic errors caused by the possible instability of detector systems. The results obtained from individual scans were found to be consistent.

$\pi^+\pi^-\gamma$ Channel

Selection of $\pi^+\pi^-\gamma$ Events

Event candidates were selected by requiring only two minimum ionizing tracks in DC and one or two photons with the energy greater than 20 MeV in the CsI calorimeter. The following selection criteria were used:

1. The average momentum of two charged particles is higher than 240 MeV/c to remove the background from $K_S \to \pi^+\pi^-$ decays.

2. Detected tracks have a polar angle between 1.05 and 2.1 radians so that they enter the inner muon system.

3. The sum of the energy depositions of two clusters associated with two tracks is less than 450 MeV to remove Bhabha events.

4. The radial distance of the closest approach of each track to the beam axis is less than 0.3 cm.

5. The Z-coordinate of the vertex (along the beam) is within 10 cm from the detector center. This cut reduces cosmic ray background by a factor of two.

6. Detected photons have a polar angle between 0.85 and 2.25 radians so that they enter the "good" region in the CsI barrel calorimeter. This requirement suppressed the background from the photons emitted by initial electrons.

7. Events with an invariant mass of two photons close to the π^0 mass $|m_{\gamma\gamma} - m_{\pi^0}| < 40$ MeV were removed.

After the above cuts the main background for the $\pi^+\pi^-\gamma$ final state comes from: a) the radiative process $e^+e^- \to \mu^+\mu^-\gamma$, b) the decay $\phi \to \pi^+\pi^-\pi^0$ when one of the photons from the π^0 escapes detection and c) collinear events $e^+e^- \to \mu^+\mu^-, \pi^+\pi^-$ in which secondary decays and interactions of muons or pions with the detector material produce a background cluster mimicking a photon.

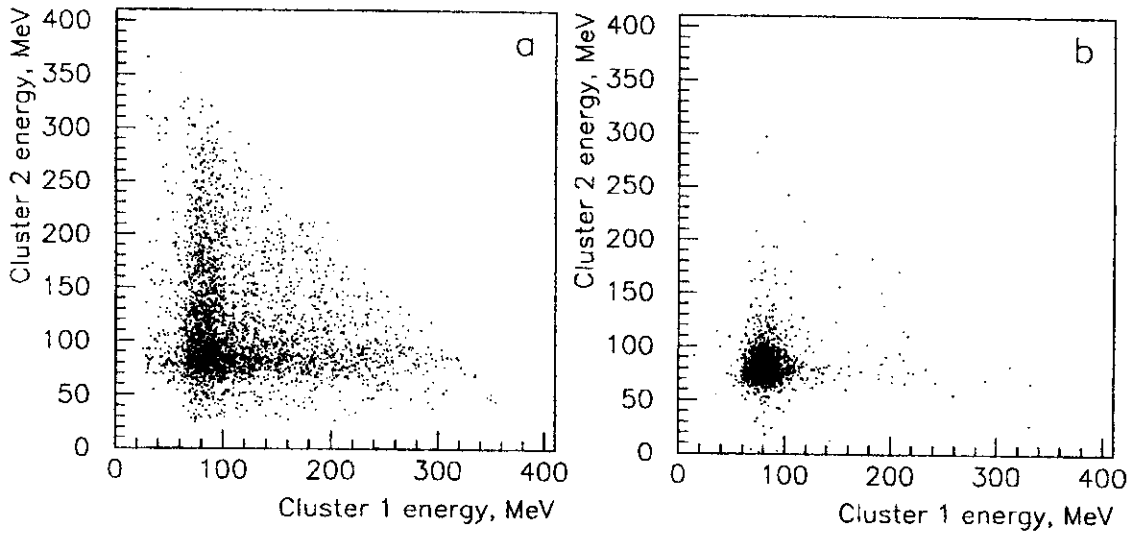

Figure 1: Calorimeter response for events with one or no hits in the muon system (a) and for events selected as muons (b).

Selection of $\mu^+\mu^-\gamma$ Events

The inner muon system was used to separate muons from pions. The requirement of hits in the inner muon system for both charged particles selects muon events, together with some pion events in which both pions pass the calorimeter without nuclear interaction.

Separation of pion and muon events in the CsI calorimeter is illustrated in Fig. 1, where scatter plots of the energy deposition of one track vs. that of the other one are presented for events with one or no hits in the muon system (a) and selected as muons (b). Energy depositions are corrected for the incident angle. Pions can have nuclear interactions and in some cases leave more energy, while muons mostly exhibit dE/dx losses only.

To select a cleaner sample of muon events, in addition to the information from the muon system both tracks were required to show only minimum ionizing energy deposition in the calorimeter (60-130 MeV). All the remaining events were considered as candidates to a pion sample. The pion sample

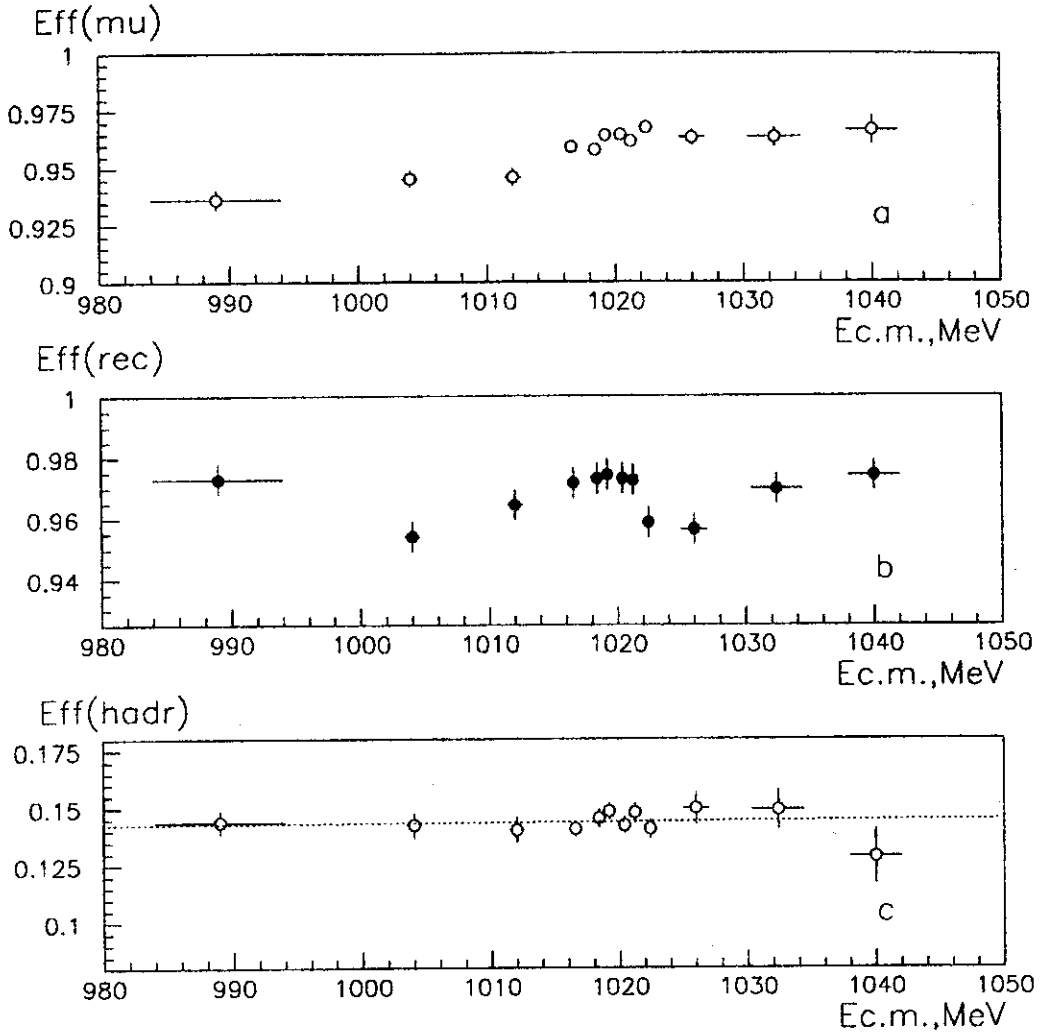

Figure 2: a.Muon system efficiency vs. energy. b.Reconstruction efficiency for DC. c.Probability for two pions to be selected as muons.

contains muons because of some inefficiency of the muon system while the muon sample contains pions since a pion can reach the muon system without nuclear interaction. The magnitudes of contamination were determined by studying correlations between the energy deposition in the CsI calorimeter and response of the muon system to collinear $\pi^+\pi^-$ and $\mu^+\mu^-$ events. The results of this study are shown in Fig. 2 for one of the experimental scans.

Figure 2a presents the muon system efficiency for different energy points. Only statistical errors are shown. The obtained number of pions and muons was corrected for the DC reconstruction efficiency shown in Fig. 2b. This efficiency was determined from collinear Bhabha events as described in [6]. The probability for two pions to be selected as muons is presented in Fig. 2c and is independent of the possible instability of the detection system. The overall systematic error in $\pi - \mu$ separation is estimated to be about 3% and

results in a correlated uncertainty in the selected number of pions and muons.

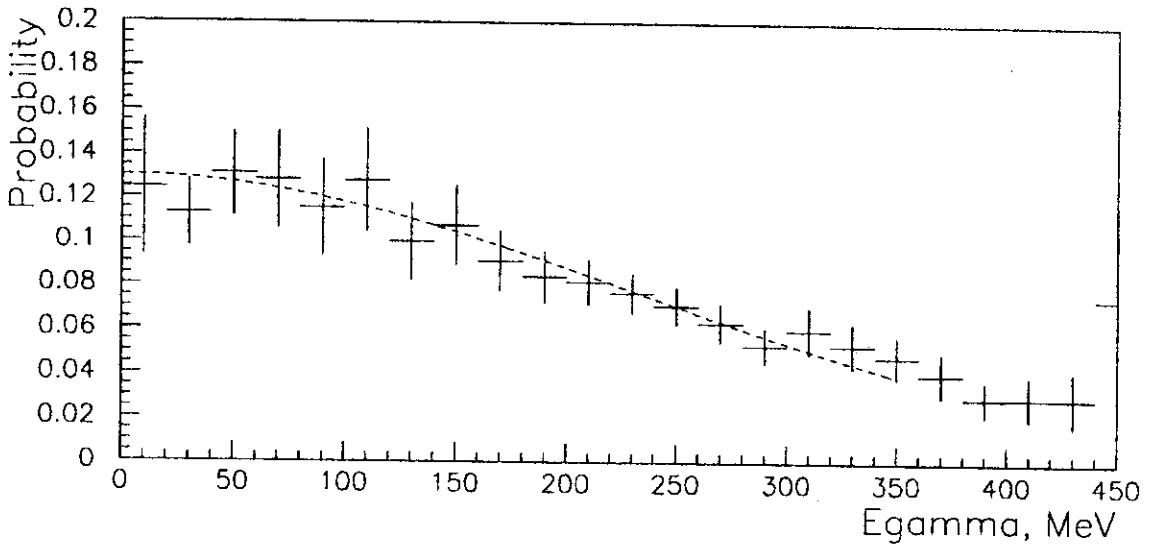

Figure 3: Simulated probability for pions to be selected as muons vs. photon energy.

For events with photons the contamination of the muon sample by pion events was studied using simulated $\pi^+\pi^-\gamma$ events. The probability of two pions to be selected as muons vs. photon energy is presented in Fig. 3 and was used for the correction of the photon spectrum. At a low photon energy this probability is consistent with that obtained from collinear events (see Fig. 2c).

Constrained Fit

To reduce the background from collinear events as well as that from the three pion annihilation a constrained fit was used requiring total energy-momentum conservation for a three body decay. About 20% of the selected events had an additional photon. In this case the constrained fit was applied to both possible combinations and that with a minimum χ^2 was chosen.

An additional cut was applied to the photon direction: an azimuthal angle should be more than 0.25 radians from the charged track direction. This cut removed the remaining collinear events with a background photon which survived after the constrained fit.

The χ^2/d.f. distribution for events selected as muons had very small background and was found to be in good agreement with simulation as shown in Fig. 4a. According to simulation a cut on the χ^2/d.f. to be less than 3

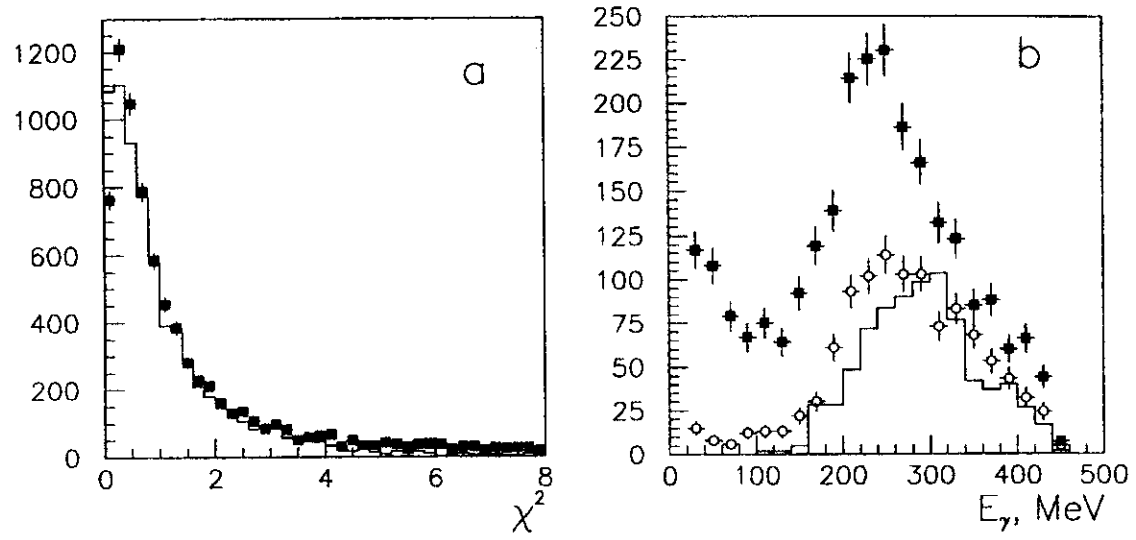

Figure 4: a. The χ^2/d.f. distribution for events selected as muons. The histogram is simulation. b. Photon spectrum for events selected as pions for χ^2/d.f.<3 (dark poins) and for $3 < \chi^2/\text{d.f.} < 6$ (open points). The histogram is simulation of background from $\pi^+\pi^-\pi^0$ events.

was imposed for pion and muon events selecting 95% of signal events.

After the above cut the pion sample still contained some background mainly from three pion decays. Such three pion background appears when one of the photons from the π^0 has the energy below 20 MeV and is not detected so that the event looks like a three body decay with the remaining photon energy higher than 150 MeV. The χ^2/d.f distribution for these events was flat and events with $3 < \chi^2/\text{d.f.} < 6$ were used to obtain the background spectrum shown in Fig. 4b by open marks. At each energy point the background spectrum was subtracted from one for the signal events.

As a result of the constrained fit one can obtain an improved estimate for the photon energy. This was studied by simulation and results are presented in Fig. 5. Simulation shows that after the constrained fit photons have energy resolution about 5 MeV in the whole energy range instead of $\sigma_{E_\gamma} = 8\% \times E_\gamma$ CsI resolution as shown in Figs. 5a,b. Figure 5c demonstrates the simulated photon detection efficiency in the CsI calorimeter vs. photon energy. The overall detector efficiency vs. photon energy for charged particles and photons is shown in Fig. 5d for $\pi^+\pi^-\gamma$ events.

Photons are required to be in the angular range 0.85-2.25 radians.

To extract the resonant contribution associated with the ϕ, two data sets

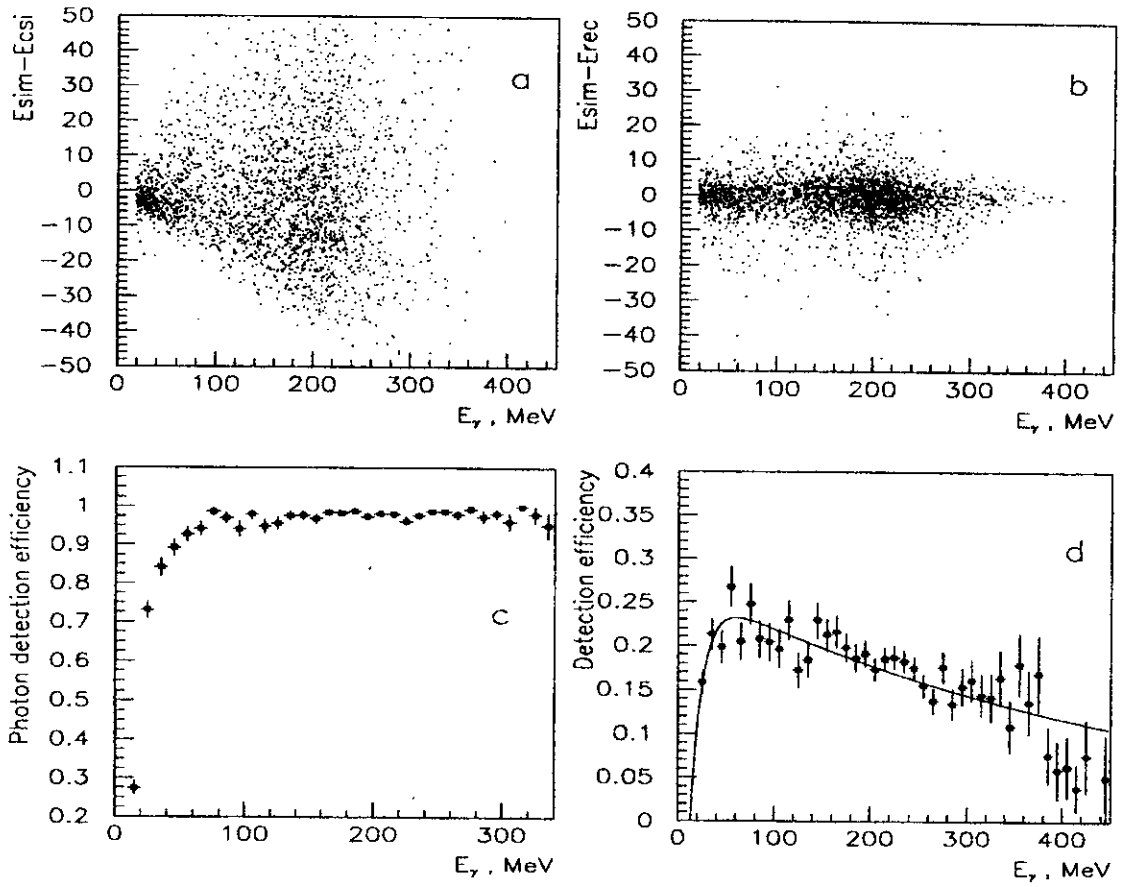

Figure 5: Study of simulated $\pi^+\pi^-\gamma$ events. a. Difference between the photon energy measured in the calorimeter and the initially simulated one vs. photon energy. b. Difference between the kinematically reconstructed photon energy and the initially simulated one vs. photon energy. c. Simulated photon detection efficiency in the CsI calorimeter. d. Overall detector efficiency vs. photon energy.

were used. Data collected at the energy points with $E_{c.m.}$ from 1016.0 to 1023.2 MeV with the integrated luminosity of 9.24 pb^{-1} were used for the "ϕ" region while those taken at $E_{c.m.}$ = 996-1013 and 1026-1060 MeV with the integrated luminosity of 3.89 pb^{-1} containing less than 3% of the ϕ decays were used for a background estimate ("off-ϕ" region).

Figures 6 present photon spectra obtained after background subtraction and corrections for the detector efficiency at the "ϕ" (a,c) and "off-ϕ" (b,d) regions for pions and muons respectively. The solid line presents theoretical calculations [9] taking into account the integrated luminosity at each energy point and $\rho - \omega$ mixing for the bremsstrahlung process. A peak at 220 MeV corresponds to the radiative process $e^+e^- \to \rho\gamma$ with the ρ decay into two

charged pions. The photon energy range from 20 to 120 MeV has minimum

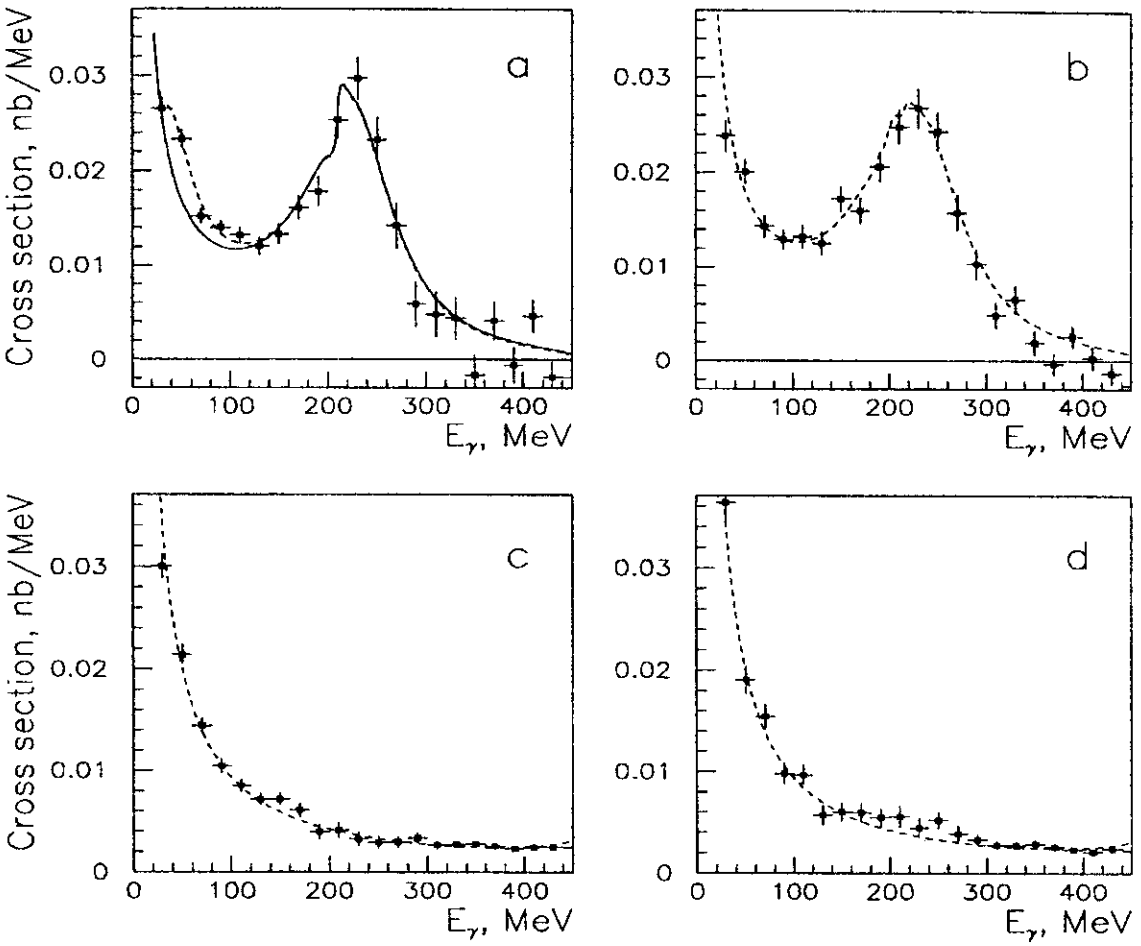

Figure 6: a. Photon spectrum for $\pi^+\pi^-\gamma$ events at the "ϕ" region; Solid line is pure bremsstrahlung. Dashed line includes a possible f_0 signal according to [9]. b. Photon spectrum for $\pi^+\pi^-\gamma$ events at the "off-ϕ" region; c,d. The same spectra for $\mu^+\mu^-\gamma$ events.

background and some excess of events over the expected bremsstrahlung spectrum can be seen in the $\pi^+\pi^-\gamma$ sample at the "ϕ" region (the dashed line in Fig. 6a). In total, 30175 $\pi^+\pi^-\gamma$ events and 27188 $\mu^+\mu^-\gamma$ events have been selected in this energy range.

Cross Section Study

The cross section for each energy point was calculated as $\sigma = N_{ev}/(\mathrm{L}\cdot\epsilon)$. N_{ev} is the number of selected events with photons in the energy range from 20 to 120 MeV. The integrated luminosity L for each energy point was determined from Bhabha events with about 2% systematic accuracy [6].

The detection efficiency ϵ was obtained by simulation and the approximation shown by the solid line in Fig. 5d was used to correct photon spectra.

The obtained cross sections of the processes $e^+e^- \to \pi^+\pi^-\gamma$ and $e^+e^- \to \mu^+\mu^-\gamma$ versus energy are presented in Fig. 7a,b. Only statistical errors are shown. The systematic error in the experimental cross sections was estimated to be about 5% dominated by the uncertainty of the pion-muon separation efficiency. The resulting cross sections contain contributions from

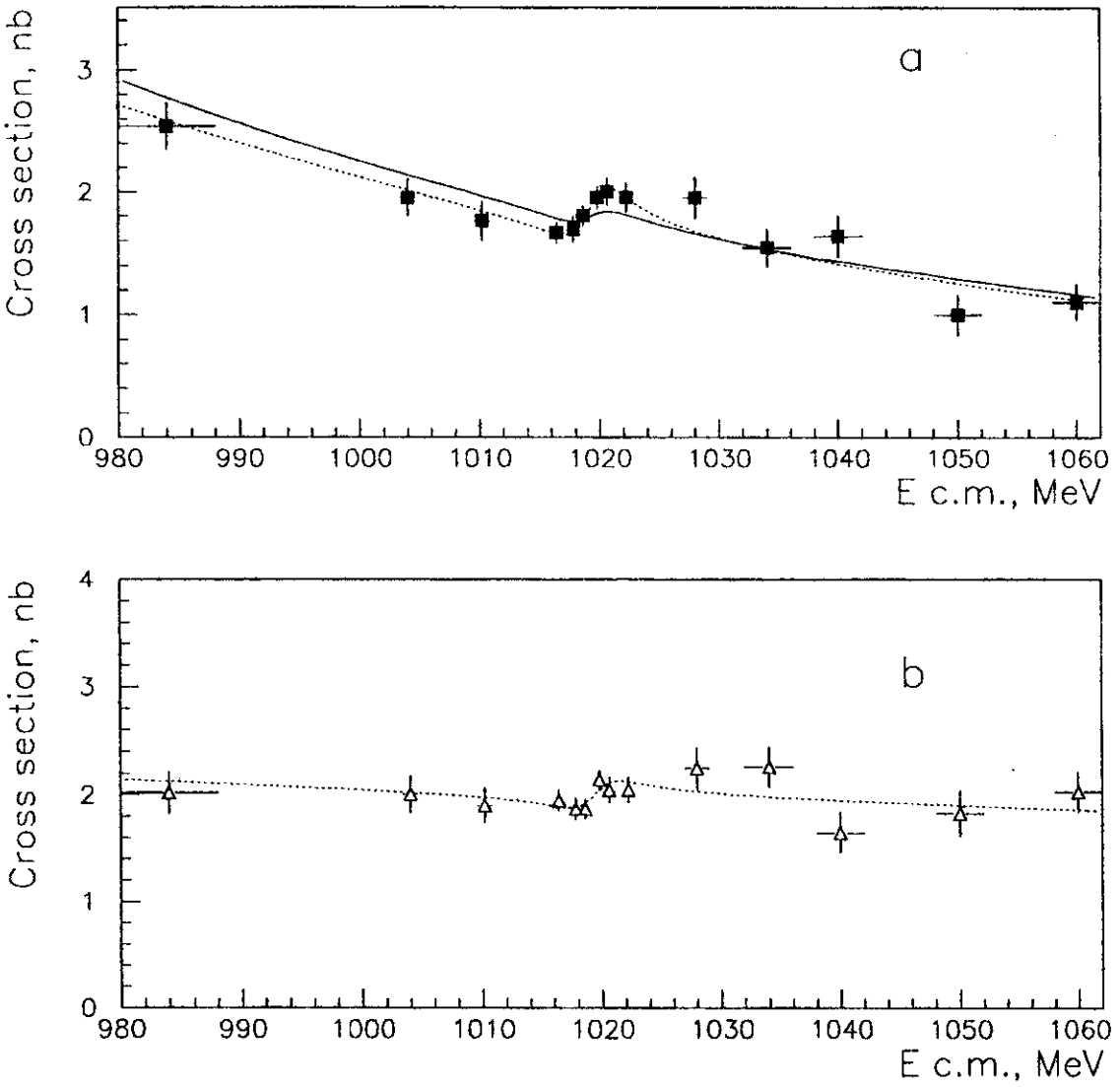

Figure 7: a. Cross section for $e^+e^- \to \pi^+\pi^-\gamma$. Lines are theoretical predictions in case of no direct ϕ decay (solid line) and best fit (dotted line). b. Cross section for $e^+e^- \to \mu^+\mu^-\gamma$ with the theoretical prediction.

bremsstrahlung by initial and final particles as well as the possible direct hadronic decay $\phi \to \pi^+\pi^-\gamma$.

The bremsstrahlung process from initial particles is suppressed by selecting photons transverse to the beam direction, but it still accounts for about 2/3 [9] of the observed $e^+e^- \to \pi^+\pi^-\gamma$ and one half of the $e^+e^- \to \mu^+\mu^-\gamma$ cross section.

The bremsstrahlung process from the final particles includes the ϕ contribution to the photon propagator (vacuum polarization). This contribution gives rise to an interference pattern in the cross section at the ϕ mass and can be referred to as an "electromagnetic" decay $\phi \to \gamma \to \pi^+\pi^-\gamma$ or $\phi \to \gamma \to \mu^+\mu^-\gamma$. The amplitude of the interference is determined by the ϕ meson leptonic coupling constant.

If the direct hadronic decay $\phi \to \pi^+\pi^-\gamma$ exists and the amplitude of this process is high enough, the interference pattern in the cross section is expected to be different from that with the vacuum polarization contribution only.

To extract the $\phi \to \pi^+\pi^-\gamma$ amplitude a simple formula has been used where the final radiation amplitude of the bremsstrahlung process is mixed with the Breit-Wigner amplitude from the ϕ:

$$\sigma(s) = \sigma_{br}^{in}(s) + \sigma_{br}^{f}(s) \cdot |1 - e^{i\psi} \cdot A_\phi \frac{m_\phi \Gamma_\phi}{\Delta_\phi}|^2;$$

$$\Delta_\phi = s - m_\phi^2 + i\sqrt{s}\Gamma_\phi(s).$$

Here $s = 4E_{beam}^2$, Γ_ϕ and m_ϕ are ϕ meson parameters, A_ϕ and ψ are the relative amplitude and phase between the bremsstrahlung and ϕ decay.

This formula is valid only if one assumes one and the same photon spectrum for the final radiation amplitude of the bremsstrahlung process and for the Breit-Wigner amplitude like for the "electromagnetic" ϕ decay.

The initial $\sigma_{br}^{in}(s)$ and final $\sigma_{br}^{f}(s)$ bremsstrahlung cross sections have different energy dependence for 20-120 MeV photons because of the pion form-factor energy behaviour. According to calculations [9] the power functions $\sigma_{br}^{in}(s) = 0.65 \cdot \sigma_0 \cdot (m_\phi/\sqrt{s})^{13}$ and $\sigma_{br}^{f}(s) = 0.35 \cdot \sigma_0 \cdot (m_\phi/\sqrt{s})^{9}$ can describe the bremsstrahlung process $e^+e^- \to \pi^+\pi^-\gamma$ in our energy range. The parameter σ_0 represents the total cross section at the ϕ mass. The function $\sigma_{br}^{in}(s) = \sigma_{br}^{f}(s) = 0.5 \cdot \sigma_0(m_\phi^2/s)$ was used for muons.

The fit of experimental data with σ_0, peak amplitude A_ϕ and ψ as free parameters shows good agreement of obtained cross sections with the theoretical calculations [9]:
$\sigma_0^{exp}/\sigma_0^{th} = 1.02 \pm 0.02 \pm 0.03$,
$\sigma_0^{exp}/\sigma_0^{th} = 0.97 \pm 0.02 \pm 0.03$

R.R.Akhmetshin, E.V.Anashkin, M.Arpagaus, V.M.Aulchenko, V.S.Banzarov, L.M.Barkov, N.S.Bashtovoy, A.E.Bondar, D.V.Bondarev, A.V.Bragin, D.V.Chernyak, A.S.Dvoretsky, S.I.Eidelman, G.V.Fedotovich, N.I.Gabyshev, A.A.Grebeniuk, D.N.Grigoriev, P.M.Ivanov, S.V.Karpov, V.F.Kazanin, B.I.Khazin, I.A.Koop, P.P.Krokovny, L.M.Kurdadze, A.S.Kuzmin, I.B.Logashenko, P.A.Lukin, A.P.Lysenko, K.Yu.Mikhailov, I.N.Nesterenko, V.S.Okhapkin, E.A.Perevedentsev, E.A.Panich, A.S.Popov, T.A.Purlatz, N.I.Root, A.A.Ruban, N.M.Ryskulov, A.G.Shamov, Yu.M.Shatunov, B.A.Shwartz, A.L.Sibidanov, V.A.Sidorov, A.N.Skrinsky, V.P.Smakhtin, I.G.Snopkov, E.P.Solodov, P.Yu.Stepanov, A.I.Sukhanov, V.M.Titov, Yu.V.Yudin, S.G.Zverev

Study of the ϕ decays into $\pi^+\pi^-\gamma$, $\pi^0\pi^0\gamma$ and $\eta\pi^0\gamma$ final states

П.П. Ахметшин, Е.В. Анашкин и др.
(всего 53 авторов)

Изучение распадов ϕ мезона в $\pi^+\pi^-\gamma$, $\pi^0\pi^0\gamma$ и $\eta\pi^0\gamma$ конечные состояния

Budker INP 99-51

Ответственный за выпуск А.М. Кудрявцев
Работа поступила 8.06.1999 г.

Сдано в набор 15.06.1999 г.
Подписано в печать 15.06.1999 г.
Формат бумаги 60×90 1/16 Объем 1.9 печ.л., 1.6 уч.-изд.л.
Тираж 150 экз. Бесплатно. Заказ N° 51

Обработано на IBM PC и отпечатано на
ротапринте ИЯФ им. Г.И. Будкера СО РАН
Новосибирск, 630090, пр. академика Лаврентьева, 11.